



Noise estimation in parallel MRI: GRAPPA and SENSE

Santiago Aja-Fernández*, Gonzalo Vegas-Sánchez-Ferrero, Antonio Tristán-Vega

LPI, ETSI Telecomunicación, Universidad de Valladolid, Spain

ARTICLE INFO

Article history:

Received 2 July 2013

Revised 17 September 2013

Accepted 1 December 2013

Keywords:

Noise estimation
Multiple-coil
Parallel imaging
SENSE
GRAPPA

ABSTRACT

Parallel imaging methods allow to increase the acquisition rate via subsampled acquisitions of the \mathbf{k} -space. SENSE and GRAPPA are the most popular reconstruction methods proposed in order to suppress the artifacts created by this subsampling. The reconstruction process carried out by both methods yields to a variance of noise value which is dependent on the position within the final image. Hence, the traditional noise estimation methods – based on a single noise level for the whole image – fail. In this paper we propose a novel methodology to estimate the spatial dependent pattern of the variance of noise in SENSE and GRAPPA reconstructed images. In both cases, some additional information must be known beforehand: the sensitivity maps of each receiver coil in the SENSE case and the reconstruction coefficients for GRAPPA.

© 2014 Elsevier Inc. All rights reserved.

1. Introduction

Magnetic Resonance Imaging (MRI) is known to be affected by several sources of quality deterioration, due to limitations in the hardware, scanning times, movement of patients, or even the motion of molecules in the scanning subject. Among them, noise is one source of degradation that affects acquisitions. The presence of noise over the acquired MR signal is a problem that affects not only the visual quality of the images, but also may interfere with further processing techniques such as registration or tensor estimation in Diffusion Tensor MRI [1].

Noise has usually been statistically modeled attending to the scanner coil architecture. For a single-coil acquisition, the complex spatial MR data are typically modeled as a complex Gaussian process, where the real and imaginary parts of the original signal are corrupted with uncorrelated Gaussian noise with zero mean and equal variance σ_n^2 . Thus, the magnitude signal is the Rician distributed envelope of the complex signal [2]. This Rician distribution whose variance is the same for the whole image is also known as *homogeneous* Rician distribution or, more accurately, *stationary* Rician distribution, and it has been the most used model in literature for multiple applications [3–8].

When a multiple-coil MR acquisition system is considered, the Gaussian process is repeated for each receiving coil. As a consequence, noise in each coil in the \mathbf{k} -space can be also modeled as a complex stationary Additive White Gaussian Noise process, with

zero mean and equal variance. In that case, the noise in the complex signal in the \mathbf{x} -space for each coil will also be Gaussian. If the \mathbf{k} -space is fully sampled, the composite magnitude signal (CMS, i.e. the final real signal after reconstruction) is obtained using methods such as the sum-of-squares (SoS) [9]. Assuming the noise components to be identically and independently distributed, the CMS will follow a non-central chi ($nc-\chi$) distribution [9]. If the correlation between coils is taken into account, the data do not strictly follow an $nc-\chi$ but, for practical purposes, it can be modeled as such, but taking into account effective parameters [10,11].

However, in multiple-coil systems, fully sampling the \mathbf{k} -space acquisition is not the common trend in acquisition. Nowadays, due to time restrictions, most acquisitions are usually accelerated by using parallel MRI (pMRI) reconstruction techniques, which allow to increase the acquisition rate via subsampled acquisitions of the \mathbf{k} -space. This acceleration goes together with an artifact known as *aliasing*.

Many reconstruction methods have been proposed in order to suppress the aliasing created by this subsampling, with SENSE (Sensitivity Encoding for Fast MRI) [12] and GRAPPA (Generalized Autocalibrating Partially Parallel Acquisition) [13] being dominant among them. From a statistical point of view, both reconstruction methods will affect the stationarity of the noise in the reconstructed data, i.e. the spatial distribution of the noise across the image. As a result, if SENSE is used, the magnitude signal may be considered Rician distributed [14,15] but the value of the statistical parameters and, in particular, the variance of noise σ_n^2 , will vary for different image locations, i.e. it becomes \mathbf{x} -dependent. Similarly, if GRAPPA is used, the CMS may be approximated by a non-stationary $nc-\chi$ distribution [15,16] with effective parameters.

* Corresponding author.

E-mail addresses: sanaja@tel.uva.es (S. Aja-Fernández), gvegsan@lpi.tel.uva.es (G. Vegas-Sánchez-Ferrero), atriveg@lpi.tel.uva.es (A. Tristán-Vega).

Noise estimators proposed in literature are based on the assumption of a single σ_n^2 value for all the pixels in the image, assuming either a Rician model [17,18,5,4,19,20] or an nc- χ [9,19,21,10]. Accordingly, those methods do not apply when dealing with pMRI and non-stationary noise. Noise estimators must therefore be reformulated in order to cope with these new image modalities.

In this paper we propose different methodologies to estimate the spatially distributed variance of noise σ_n^2 from the magnitude signal when SENSE or GRAPPA are used as pMRI technique.

2. Noise statistical models in pMRI

As previously stated, most noise estimation methods in literature rely on the assumption of a single value of σ_n^2 for every pixel within the image. However, this is no longer the case when pMRI protocols are considered.

In multiple coil systems, the acquisition rate may be increased by subsampling the \mathbf{k} -space data [22,23], while reducing phase distortions when strong magnetic field gradients are present. The immediate effect of the \mathbf{k} -space subsampling is the appearance of aliased replicas in the image domain retrieved at each coil. In order to suppress or correct this aliasing, pMRI combines the redundant information from several coils to reconstruct a single non-aliased image domain.

The commonly used (stationary) Rician and nc- χ models do not necessarily hold in this case. Depending on the way the information from each coil is combined, the statistics of the image will follow different distributions. It is therefore necessary to study the behavior of the data for a particular reconstruction method. We will focus on two of the most popular methods, SENSE [12] and GRAPPA [13], in their most basic formulation.

In the following sections we will assume an L -coil configuration, with L being the number of coils in the system. $s_l^S(\mathbf{k})$ is the subsampled signal at the l -th coil of the \mathbf{k} -space ($l = 1, \dots, L$), $S_l^S(\mathbf{x})$ is the subsampled signal in the image domain, i.e., the \mathbf{x} -space, and r is the subsampling rate. The \mathbf{k} -space data at each coil can be accurately described by an Additive White Gaussian Noise (AWGN) process, with zero mean and variance $\sigma_{K_l}^2$:

$$s_l^S(\mathbf{k}) = a_l(\mathbf{k}) + n_l(\mathbf{k}; \sigma_{K_l}^2), \quad l = 1, \dots, L \tag{1}$$

with $a_l(\mathbf{k})$ the noise-free signal and $n_l(\mathbf{k}; \sigma_{K_l}^2) = n_{l_r}(\mathbf{k}; \sigma_{K_l}^2) + j \cdot n_{l_i}(\mathbf{k}; \sigma_{K_l}^2)$ the AWGN process, which is initially assumed stationary so that $\sigma_{K_l}^2$ does not depend on \mathbf{k} .

The complex \mathbf{x} -space is obtained as the inverse Discrete Fourier Transform (iDFT) of $s_l^S(\mathbf{k})$ for each slice or volume, so the noise in the complex \mathbf{x} -space is still Gaussian [15]:

$$S_l^S(\mathbf{x}) = A_l(\mathbf{x}) + N_l(\mathbf{x}; \sigma_l^2), \quad l = 1, \dots, L$$

where $N_l(\mathbf{x}; \sigma_l^2) = N_{l_r}(\mathbf{x}; \sigma_l^2) + jN_{l_i}(\mathbf{x}; \sigma_l^2)$ is also a complex AWGN process (note we are assuming that there are not any spatial correlations) with zero mean and covariance matrix:

$$\Sigma = \begin{pmatrix} \sigma_1^2 & \sigma_{12} & \dots & \sigma_{1L} \\ \sigma_{21} & \sigma_2^2 & \dots & \sigma_{2L} \\ \vdots & \vdots & \ddots & \vdots \\ \sigma_{L1} & \sigma_{L2} & \dots & \sigma_L^2 \end{pmatrix}. \tag{2}$$

The relation between the noise variances in the \mathbf{k} - and \mathbf{x} -domains is given by the number of points used for the iDFT:

$$\sigma_l^2 = \frac{r}{|\Omega|} \sigma_{K_l}^2,$$

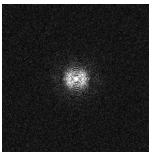
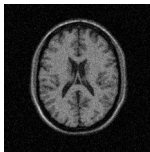
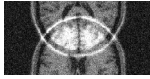
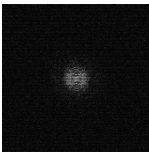
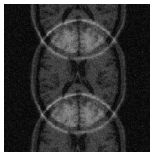
with $|\Omega|$ the final number of pixels in the field of view (FOV). Note that the final noise power is greater than in the fully sampled case due to the reduced \mathbf{k} -space averaging, as it will be the case with SENSE (see below). On the contrary, the iDFT may be computed after zero-padding the missing (not sampled) \mathbf{k} -space lines, and then we have [16]:

$$\sigma_l^2 = \frac{1}{|\Omega| \cdot r} \sigma_{K_l}^2.$$

In the latter case the noise power is reduced with respect to the fully sampled case, since we average exactly the same number of samples but only 1 of each r of them contributes a noise sample (this will also be the case with GRAPPA). Finally, note that although the level of noise is smaller in GRAPPA due to the zero padding, the SNR does not increase, since the zero padding produces also a reduction of the level of the signal.

Relations between the variance of noise in complex \mathbf{x} -space and \mathbf{k} -space for each coil are summarized in Table 1.

Table 1
Relations between the variance of noise in complex MR data for each coil in the \mathbf{k} -space and the image domain.

Noise relations			
\mathbf{k} -space	Parameters	\mathbf{x} -space	Relation
	Fully sampled, $\sigma_{K_l}^2$, \mathbf{k} -size: $ \Omega $		$\sigma_l^2 = \frac{1}{ \Omega } \sigma_{K_l}^2$, \mathbf{x} -size: $ \Omega $
	Subsampled r , $\sigma_{K_l}^2$, \mathbf{k} -size: $ \Omega /r$		$\sigma_l^2 = \frac{r}{ \Omega } \sigma_{K_l}^2$, \mathbf{x} -size: $ \Omega /r$ (SENSE)
	Subsampled r , $\sigma_{K_l}^2$, \mathbf{k} -size: $ \Omega $ (zero padded)		$\sigma_l^2 = \frac{1}{ \Omega \cdot r} \sigma_{K_l}^2$, \mathbf{x} -size: $ \Omega $ (GRAPPA)

2.1. Statistical Noise Model in SENSE Reconstructed Images

Prior to the definition of the estimators, the statistical noise model in SENSE must be properly defined. Many studies have been made about this topic from an SNR or a g -factor (noise amplification) point of view [12,15,24]. Since this paper is focused on the σ_n^2 value estimation rather than an SNR level, an equivalent reformulation must be done, more coherent with the signal and noise analysis usually assumed for noise estimation.

In multiple coil scanners, the signal acquired in each coil, $l = 1, 2, \dots, L$, can be modeled in the \mathbf{k} -space by the following equation [22,25]:

$$s_l(\mathbf{k}) = \int_V C_l(\mathbf{x}) S_0(\mathbf{x}) e^{j2\pi \mathbf{k} \cdot \mathbf{x}} d\mathbf{x},$$

where $S_0(\mathbf{x})$ is the excited spin density function throughout the volume V (it is sometime denoted by $\rho(\mathbf{x})$), and it can be seen as an *original image* weighted by the spatial sensitivity of coil l -th, $C_l(\mathbf{x})$. In the \mathbf{x} -space this is equivalent to [22,26]:

$$S_l(\mathbf{x}) = C_l(\mathbf{x}) S_0(\mathbf{x}), \quad l = 1, \dots, L. \quad (3)$$

An accelerated pMRI acquisition with a factor r will reduce the matrix size of the image at every coil. The signal in one pixel at location (x, y) of l -th coil can be now written as [12,26]:

$$S_l(x, y) = C_l(x, y_1) S_0(x, y_1) + \dots + C_l(x, y_r) S_0(x, y_r). \quad (4)$$

Let us call $S_l^S(x, y)$ to the subsampled signal at coil l -th and $S^R(x, y)$ to the final reconstructed image. Note that the latter can be seen as an estimator of the original image $S^R(x, y) = \widehat{S}_0(x, y)$ that can be obtained from Eq. (4)

$$\begin{aligned} S_l^S(x, y) &= C_l(x, y_1) \widehat{S}_0^S(x, y_1) + \dots + C_l(x, y_r) \widehat{S}_0^S(x, y_r) \\ &= C_l(x, y_1) S^R(x, y_1) + \dots + C_l(x, y_r) S^R(x, y_r) \quad l = 1, \dots, L \end{aligned}$$

$S^R(x, y)$ can be easily derived from this relation. For instance, for $r = 2$ for pixel (x, y) , $S^R(x, y)$ becomes [12,22,26]

$$\begin{bmatrix} S_1^R \\ S_2^R \end{bmatrix} = [\mathbf{W}_1 \quad \mathbf{W}_2] \times [S_1^S \quad \dots \quad S_L^S], \quad (5)$$

where S_i^R stands for each of the r reconstructed pixels. In matrix form for each pixel and an arbitrary r

$$S_i^R = \mathbf{W}_i \times \mathbf{S}^S \quad i = 1, \dots, r, \quad (6)$$

with $\mathbf{W} = [\mathbf{W}_1, \dots, \mathbf{W}_r]$ a reconstruction matrix created from the sensitivity maps at each coil. These maps, $\mathbf{C} = [\mathbf{C}_1, \dots, \mathbf{C}_L]$ are estimated through calibration right before each acquisition session. Once they are known, the matrix \mathbf{W} reduces to a least-squares solver for the overdetermined problem $\mathbf{C}(x, y) \times \mathbf{S}^R(x, y) \approx \mathbf{S}^S(x, y)$ [12,26]:

$$\mathbf{W}(x, y) = (\mathbf{C}^*(x, y) \mathbf{C}(x, y))^{-1} \mathbf{C}^*(x, y). \quad (7)$$

The correlation between coils may be incorporated in the reconstruction as a pre-whitening matrix for the measurements, and $\mathbf{W}(x, y)$ becomes then a weighted least squares solver with correlation matrix $\mathbf{\Sigma}$:

$$\mathbf{W}(x, y) = (\mathbf{C}^*(x, y) \mathbf{\Sigma}^{-1} \mathbf{C}(x, y))^{-1} \mathbf{C}^*(x, y) \mathbf{\Sigma}^{-1}.$$

The SNRs of the fully sampled image and the image reconstructed with SENSE are related by the so-called g -factor, g [24,26]:

$$\text{SNR}_{\text{SENSE}} = \frac{\text{SNR}_{\text{full}}}{\sqrt{r} \cdot g} \quad (8)$$

However, in our problem we are more interested on the actual noise model underlying the SENSE reconstruction and on the final variance of noise. The final signal S_l^R is obtained as a linear combination of S_l^S , where the noise is Gaussian distributed. Thus, the resulting signal is also Gaussian, with variance:

$$\sigma_i^2 = \mathbf{W}_i^* \mathbf{\Sigma} \mathbf{W}_i. \quad (9)$$

Since \mathbf{W}_i is position-dependent, i.e. $\mathbf{W}_i = \mathbf{W}_i(x, y)$, so will be the variance of noise, $\sigma_i^2(x, y)$. For further reference, when the whole image is taken into account, let us denote the variance of noise for each pixel in the reconstructed data by $\sigma_R^2(\mathbf{x})$.

All in all, noise in the final reconstructed signal $S^R(x, y)$ will follow a complex Gaussian distribution. If the magnitude is considered, i.e. $M(x, y) = |S^R(x, y)|$, the final magnitude image will follow a Rician distribution [15], just like single-coil systems.

To sum up: (1) Subsampled multi coil MR data reconstructed with Cartesian SENSE follow a Rician distribution at each point of the image; (2) The resulting distribution is non-stationary. This means that the variance of noise will vary from point to point across the image; (3) The final value of the variance of noise at each point will only depend on the covariance matrix of the original data (prior to reconstruction) and on the sensitivity map, and not on the data themselves.

2.2. Noise statistical model in GRAPPA

The GeneRALized Autocalibrated Partially Parallel Acquisitions (GRAPPA) [13] reconstruction strategy estimates the full \mathbf{k} -space in each coil from a sub-sampled \mathbf{k} -space acquisition. The reconstructed lines are estimated through a linear combination of the existing samples. Weighted data in a neighborhood $\eta(\mathbf{k})$ around the estimated pixel from several coils are used for such an estimation. While the sampled data $s_l^S(\mathbf{k})$ remain the same, the reconstructed lines $S_l^R(\mathbf{k})$ are estimated through a linear combination of the existing samples. Weighted data in a neighborhood $\eta(\mathbf{k})$ around the estimated pixel from several coils are used for such an estimation:

$$s_l^R(\mathbf{k}) = \sum_{m=1}^L \sum_{\mathbf{c} \in \eta(\mathbf{k})} s_m^S(\mathbf{k} - \mathbf{c}) \omega_m(l, \mathbf{c}), \quad (10)$$

with $s_l(\mathbf{k})$ the complex signal from coil l at point \mathbf{k} and $\omega_m(l, \mathbf{k})$ the complex reconstruction coefficients for coil l . These coefficients are determined from the low-frequency coordinates of \mathbf{k} -space, termed the Auto Calibration Signal (ACS) lines, which are sampled at the Nyquist rate (i.e. unaccelerated). Breuer et al. [27] pointed out that Eq. (10) can be rewritten using the *convolution* operator:

$$s_l^R(\mathbf{k}) = \sum_{m=1}^L s_m^S(\mathbf{k}) \otimes w_m(l, \mathbf{k}), \quad (11)$$

where $w_m(l, \mathbf{k})$ is a convolution kernel that can be easily derived from the GRAPPA weight set $\omega_m(l, \mathbf{k})$. Since a (circular) convolution in the \mathbf{k} -space is equivalent to a product into the \mathbf{x} -space, we can write:

$$S_l^R(\mathbf{x}) = |\Omega| \sum_{m=1}^L S_m^S(\mathbf{x}) \times W_m(l, \mathbf{x}),$$

with $W_m(l, \mathbf{x})$ the GRAPPA reconstruction coefficients in the \mathbf{x} -space and $|\Omega|$ the size of the image in each coil.

The CMS can be obtained using the SoS of the signal in each coil:

$$M_L(\mathbf{x}) = \sqrt{\sum_{l=1}^L |S_l^R(\mathbf{x})|^2}. \quad (12)$$

In [16] the authors pointed out that the resultant distribution of the CMS in Eq. (12) is not strictly a nc- χ , but its behavior will be very similar and could be modeled as such with a small approximation error. However, the reconstruction method will highly increase the correlations between the reconstructed signals in each coil, which translates into a decrease of the number of Degrees of Freedom of the distribution. As a consequence, the final distribution will show a (reduced) *effective number of coils* L_{eff} and an (increased) *effective variance of noise* σ_{eff}^2 :

$$L_{\text{eff}}(\mathbf{x}) = \frac{|\mathbf{A}|^2 \text{tr}(\mathbf{C}_X^2) + (\text{tr}(\mathbf{C}_X^2))^2}{\mathbf{A}^* \mathbf{C}_X^2 \mathbf{A} + \|\mathbf{C}_X^2\|_F^2}, \quad (13)$$

$$\sigma_{\text{eff}}^2(\mathbf{x}) = \frac{\text{tr}(\mathbf{C}_X^2)}{L_{\text{eff}}}, \quad (14)$$

where $\mathbf{C}_X^2(\mathbf{x}) = \mathbf{W}\mathbf{\Sigma}\mathbf{W}^*$ is the covariance matrix of the *interpolated* data at each spatial location, $\mathbf{A}(\mathbf{x}) = [A_1, \dots, A_L]^T$ is the noise-free reconstructed signal, $\|\cdot\|_F$ is the Frobenius norm, $\mathbf{\Sigma}$ is the covariance matrix of the *original* data and $\mathbf{W}(\mathbf{x})$ is the GRAPPA interpolation matrix for each (\mathbf{x}) :

$$\mathbf{W}(\mathbf{x}) = \begin{pmatrix} W_1(1, \mathbf{x}) & \dots & W_1(L, \mathbf{x}) \\ \vdots & \ddots & \vdots \\ W_L(1, \mathbf{x}) & \dots & W_L(L, \mathbf{x}) \end{pmatrix}$$

Although the nc- χ model is feasible for GRAPPA, the resulting distribution is non-stationary since the effective parameters are spatially dependent.

2.3. Practical simplifications over the GRAPPA model

For practical purposes, in order to make the noise estimation feasible, some simplifications can be made over Eqs. (13) and (14). We will simplify the problem by assuming that the variance of noise is the same for every coil, $\sigma_l^2 = \sigma_n^2$, and that the signal is also the same $A_i = A_j$ for all i, j . The covariance matrix can therefore be written as:

$$\mathbf{\Sigma} = \sigma_n^2 \cdot \begin{pmatrix} 1 & \rho_{12} & \dots & \rho_{1L} \\ \rho_{21} & 1 & \dots & \rho_{2L} \\ \vdots & \vdots & \ddots & \vdots \\ \rho_{L1} & \rho_{L2} & \dots & 1 \end{pmatrix}. \quad (15)$$

Accordingly, matrix \mathbf{C}_X^2 becomes

$$\mathbf{C}_X^2(\mathbf{x}) = \sigma_n^2 \cdot \mathbf{W} \times \begin{pmatrix} 1 & \rho_{12} & \dots & \rho_{1L} \\ \rho_{21} & 1 & \dots & \rho_{2L} \\ \vdots & \vdots & \ddots & \vdots \\ \rho_{L1} & \rho_{L2} & \dots & 1 \end{pmatrix} \times \mathbf{W}^* = \sigma_n^2 \cdot \mathbf{\Theta}(\mathbf{x}). \quad (16)$$

The effective values may be now simplified to:

$$L_{\text{eff}}(\mathbf{x}) = \frac{\text{SNR}^2 L \text{tr}(\mathbf{\Theta}) + (\text{tr}(\mathbf{\Theta}))^2}{\text{SNR}^2 \|\mathbf{\Theta}\|_1 + \|\mathbf{\Theta}\|_F^2}, \quad (17)$$

$$\sigma_{\text{eff}}^2(\mathbf{x}) = \sigma_n^2 \frac{\text{SNR}^2 \|\mathbf{\Theta}\|_1 + \|\mathbf{\Theta}\|_F^2}{\text{SNR}^2 L + \text{tr}(\mathbf{\Theta})}, \quad (18)$$

with $\text{SNR}^2(\mathbf{x}) = \frac{A_i^2(\mathbf{x})}{L\sigma_n^2}$. For these equations, two extreme cases can be considered:

1. In the background, where no signal is present and hence $\text{SNR} = 0$, the effective values are:

$$L_{\text{eff},B} = \frac{(\text{tr}(\mathbf{\Theta}))^2}{\|\mathbf{\Theta}\|_F^2} \quad (19)$$

$$\sigma_{\text{eff},B}^2 = \sigma_n^2 \frac{\|\mathbf{\Theta}\|_F^2}{\text{tr}(\mathbf{\Theta})}. \quad (20)$$

2. For high SNR areas, say $\text{SNR} \rightarrow \infty$:

$$L_{\text{eff},S} = L \cdot \frac{\text{tr}(\mathbf{\Theta})}{\|\mathbf{\Theta}\|_1} \quad (21)$$

$$\sigma_{\text{eff},S}^2 = \sigma_n^2 \frac{\|\mathbf{\Theta}\|_1}{L}. \quad (22)$$

These two cases give respectively the lower and upper bounds of $\sigma_{\text{eff}}^2(\mathbf{x})$ within the image (vice-versa for L_{eff}). Using the simplified version of the effective variance of noise in Eq. (22) we can write:

$$\sigma_{\text{eff}}^2(\mathbf{x}) = \phi_n(\mathbf{x}) \cdot \sigma_{\text{eff},B}^2 + (1 - \phi_n(\mathbf{x})) \cdot \sigma_{\text{eff},S}^2 \quad (23)$$

with

$$\phi_n(\mathbf{x}) = \frac{\text{tr}(\mathbf{\Theta}(\mathbf{x}))}{L \text{SNR}^2(\mathbf{x}) + \text{tr}(\mathbf{\Theta}(\mathbf{x}))}. \quad (24)$$

Note that $\phi_n(\mathbf{x})$ becomes 1 in the background (when $\text{SNR} \rightarrow 0$) and becomes 0 in high SNR areas (when $\text{SNR} \rightarrow \infty$).

The simplified model here presented is far from the *standard* stationary nc- χ generally used, and clearly very far from the stationary Rician model. If we consider results in Eqs. (20) and (22) we can see that the variance of noise in the background and in the signal areas will be different. If the estimation of noise is done using only the background (as it has been traditionally done) and no corrections are done, there will be a bias when used over the signal areas.

3. Noise estimation

3.1. Noise Estimation in SENSE

In the background of a SENSE MR image, where the SNR is zero, the Rician PDF simplifies to a (non-stationary) Rayleigh distribution, whose second order moment is defined as

$$E\{M^2(\mathbf{x})\} = 2 \cdot \sigma_R^2(\mathbf{x}). \quad (25)$$

Since $\sigma_R^2(\mathbf{x})$ is \mathbf{x} -dependent, $E\{M^2(\mathbf{x})\}$ will also show a different value for each \mathbf{x} position.

Let us assume that each coil in the \mathbf{x} -space is initially corrupted with uncorrelated Gaussian noise with the same variance σ_n^2 and there is a correlation between coils ρ so that matrix $\mathbf{\Sigma}$ becomes

$$\mathbf{\Sigma} = \sigma_n^2 \begin{pmatrix} 1 & \rho & \dots & \rho \\ \rho & 1 & \dots & \rho \\ \vdots & \vdots & \ddots & \vdots \\ \rho & \rho & \dots & 1 \end{pmatrix} = \sigma_n^2 (\mathbf{I} + \rho[\mathbf{1} - \mathbf{I}]).$$

with \mathbf{I} the $L \times L$ identity matrix and $\mathbf{1}$ a $L \times L$ matrix of 1's. For each \mathbf{x} value, we define the global map

$$\mathcal{G}_{W_i} = \mathbf{W}_i^* (\mathbf{I} + \rho[\mathbf{1} - \mathbf{I}]) \mathbf{W}_i, \quad i = 1, \dots, r$$

Global map $\mathcal{G}_W(\mathbf{x})$ can be easily inferred from the \mathcal{G}_{W_i} values. Note that $\mathcal{G}_W(\mathbf{x})$ is strongly related to the g-factor [24]. Eq. (25) then becomes

$$E\{M^2(\mathbf{x})\} = 2 \sigma_n^2 \mathcal{G}_W(\mathbf{x}) \quad (26)$$

and

$$\sigma_n^2 = \frac{E\{M^2(\mathbf{x})\}}{2 \mathcal{G}_W(\mathbf{x})} \quad (27)$$

By using this regularization, we can assure a single σ_n^2 value for all the points in the image. Following the noise estimation philosophy in [4,19], we can now define a noise estimator based on the local sample estimation of the second order moment:

$$\langle M^2(\mathbf{x}) \rangle_{\mathbf{x}} = \frac{1}{|\eta(\mathbf{x})|} \sum_{\mathbf{p} \in \eta(\mathbf{x})} M^2(\mathbf{p}),$$

with $\eta(\mathbf{x})$ a neighborhood centered in \mathbf{x} . $\langle M^2(\mathbf{x}) \rangle_{\mathbf{x}}$ is known to follow a Gamma distribution [19] whose mode is $2\sigma_n^2(|\eta(\mathbf{x})| - 1)/|\eta(\mathbf{x})|$. Then

$$\text{mode} \left\{ \frac{\langle M_L^2(\mathbf{x}) \rangle_{\mathbf{x}}}{\mathcal{G}_W(\mathbf{x})} \right\} = 2\sigma_n^2 \frac{|\eta(\mathbf{x})| - 1}{|\eta(\mathbf{x})|} \approx 2\sigma_n^2$$

when $|\eta(\mathbf{x})| \gg 1$. The estimator is then defined as

$$\widehat{\sigma}_n^2 = \frac{1}{2} \text{mode} \left\{ \frac{\langle M_L^2(\mathbf{x}) \rangle_{\mathbf{x}}}{\mathcal{G}_W(\mathbf{x})} \right\} \quad (28)$$

and consequently the noise in each pixel is estimated as

$$\widehat{\sigma}_R^2(\mathbf{x}) = \frac{1}{2} \text{mode} \left\{ \frac{\langle M_L^2(\mathbf{x}) \rangle_{\mathbf{x}}}{\mathcal{G}_W(\mathbf{x})} \right\} \mathcal{G}_W(\mathbf{x}) \quad (29)$$

This estimator is only valid over the background pixels. However, as shown in [4,19], no segmentation of these pixels is needed: the

use of the mode allows us to work with the whole image. On the other hand, to carry out the estimation, the sensitivity map of each coil and the correlation between coils must be known beforehand. These parameters are needed for the SENSE encoding, and thus, they can be easily obtained.

3.2. Noise estimation in GRAPPA

The background area of a GRAPPA reconstructed image may be approximated by a $c\text{-}\chi$ distribution, whose second order moment is defined as

$$E\{M_L^2\} = 2\sigma_n^2 L. \quad (30)$$

Effective parameters $L_{\text{eff}}(\mathbf{x})$ and $\sigma_{\text{eff}}^2(\mathbf{x})$ must be taken into account. Since both are \mathbf{x} -dependent, $E\{M_L^2\}$ will also show a different value for each \mathbf{x} position:

$$E\{M_L^2(\mathbf{x})\} = 2 \sigma_{\text{eff}}^2(\mathbf{x}) L_{\text{eff}}(\mathbf{x}) = 2 \text{tr}(\mathbf{C}_X^2(\mathbf{x}))$$

and assuming the simplifications proposed in Section 2.3:

$$E\{M_L^2(\mathbf{x})\} = 2 \sigma_n^2 \text{tr}(\mathbf{\Theta}(\mathbf{x})).$$

In order to estimate a possible value of σ_n^2 matrices $\mathbf{W}(\mathbf{x})$ (the GRAPPA weights) must be known before hand. In addition, some assumption must be also made over covariance matrix $\mathbf{\Sigma}$. One possible assumption is the same correlation between all coils, as done in SENSE:

$$\mathbf{\Sigma} = \sigma_n^2 \begin{pmatrix} 1 & \rho & \dots & \rho \\ \rho & 1 & \dots & \rho \\ \vdots & \vdots & \ddots & \vdots \\ \rho & \rho & \dots & 1 \end{pmatrix} = \sigma_n^2 (\mathbf{I} + \rho[\mathbf{1} - \mathbf{I}]).$$

or, in a much simplified case, no correlations between coils, $\mathbf{\Sigma} = \sigma_n^2 \mathbf{I}$. In any case, from Eq. (30) we can always derive

$$\sigma_n^2 = \frac{E\{M_L^2(\mathbf{x})\}}{2 \text{tr}(\mathbf{\Theta}(\mathbf{x}))} \quad (31)$$

Following the same noise estimation philosophy proposed for SENSE, we can define a noise estimator based on the local sample estimation of the second order moment:

$$\widehat{\sigma}_n^2 = \frac{1}{2} \text{mode} \left\{ \frac{\langle M_L^2(\mathbf{x}) \rangle_{\mathbf{x}}}{\text{tr}(\mathbf{\Theta}(\mathbf{x}))} \right\} \quad (32)$$

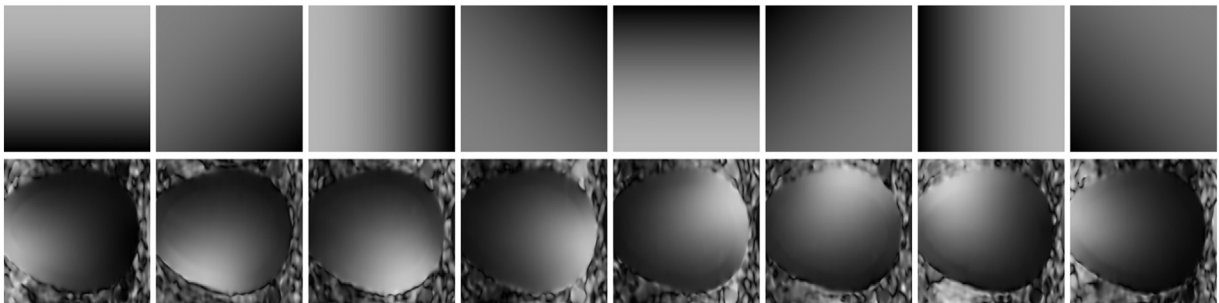


Fig. 1. Sensitivity Maps used for the experiments. Top: synthetic sensitivity map. Bottom: Map estimated from real acquisition.

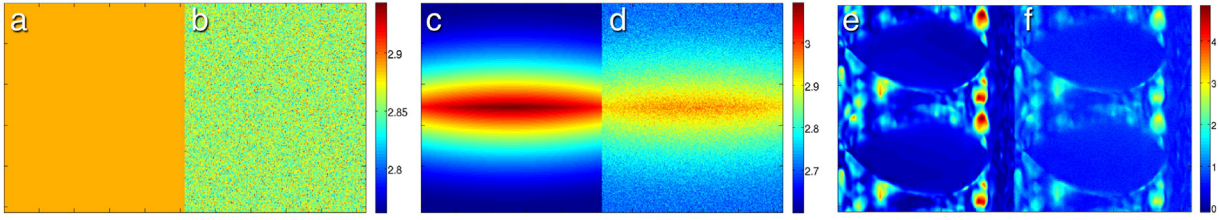


Fig. 2. Maps of $\sigma_{\mathcal{R}}^2(\mathbf{x})$ in the final image: (a–c–e): Theoretical values. (b–d–f): Estimated from samples. (a–b) Synthetic Sensitivity Map with no correlation. (c–d) Synthetic Sensitivity Map with correlation between coils. (e–f) Real sensitivity map with correlation between coils (log scale).

This estimator is only valid over the background pixels. However, as shown in [4,19], no segmentation of these pixels is needed. On the other hand, to carry out the estimation, the GRAPPA interpolation weights must be known beforehand.

3.3. Estimation of effective values in GRAPPA

Although many methods and applications based on the nc- χ use only the σ_n^2 value, there are other situations in which the effective value of noise is needed. Note that this effective value will now be \mathbf{x} -dependent.

Assuming that we know the GRAPPA weights beforehand, we can use the estimation $\widehat{\sigma}_n^2$ in Eq. (28) to estimate $\widehat{\sigma}_{n,B}^2$ and $\widehat{\sigma}_{n,S}^2$, using Eqs. (20) and (22) respectively. These two values give the lower and upper bounds of the actual $\sigma_{\text{eff}}^2(\mathbf{x})$ across the image. Using the simplified version of the effective variance of noise in Eq. (23):

$$\widehat{\sigma}_{\text{eff}}^2(\mathbf{x}) = \widehat{\phi}_n(\mathbf{x}) \cdot \widehat{\sigma}_{\text{eff},B}^2 + (1 - \widehat{\phi}_n(\mathbf{x})) \cdot \widehat{\sigma}_{\text{eff},S}^2 \quad (33)$$

A rough estimation of $\phi_n(\mathbf{x})$ can be done using the sample second order moment (although more complex estimation could also be considered). Since

$$E\{M_L^2(\mathbf{x})\} = A_T^2 + 2 \sigma_n^2 \text{tr}(\Theta(\mathbf{x})).$$

we can write

$$\begin{aligned} \phi_n &= \frac{\text{tr}(\Theta)}{\frac{A_T^2}{\sigma_n^2} + \text{tr}(\Theta)} \\ &= \frac{\text{tr}(\Theta) \sigma_n^2}{A_T^2 + \text{tr}(\Theta) \sigma_n^2} \end{aligned}$$

Therefore, a simple estimation would be

$$\widehat{\phi}_n(\mathbf{x}) = \frac{\text{tr}(\Theta) \widehat{\sigma}_n^2}{\langle M^2 \rangle - \text{tr}(\Theta) \widehat{\sigma}_n^2}. \quad (34)$$

Finally, the estimated effective noise variance becomes:

$$\widehat{\sigma}_{\text{eff}}^2(\mathbf{x}) = \widehat{\sigma}_n^2 \left[\frac{\text{tr}(\Theta) \widehat{\sigma}_n^2}{\langle M^2 \rangle - \text{tr}(\Theta) \widehat{\sigma}_n^2} \cdot \frac{\|\Theta\|_1}{L} + \left(1 - \frac{\text{tr}(\Theta) \widehat{\sigma}_n^2}{\langle M^2 \rangle - \text{tr}(\Theta) \widehat{\sigma}_n^2} \right) \cdot \frac{\|\Theta\|_F^2}{\text{tr}(\Theta)} \right]. \quad (35)$$

4. Experiments and Results

For the sake of validation of the noise estimators proposed, some experiments are carried out. We will focus first in SENSE and later in GRAPPA.

4.1. Noise estimation in SENSE

We will **first** test the variation of parameter $\sigma_{\mathcal{R}}^2(\mathbf{x})$ across the image in SENSE. To that end, we work with two sensitivity maps belonging to 8-coil systems as shown in Fig. 1: one synthetic sensitivity map (top) and a real map (bottom), estimated from a T1 acquisition done in a GE Signa 1.5 T EXCITE, FSE pulse sequence, 8 coils, TR = 500 ms, TE = 13.8 ms, 256×256 and FOV: $20 \text{ cm} \times 20 \text{ cm}$. For the sake of simplicity we assume a normalized variance at each coil $\sigma_i^2 = 1$ since it will not affect the experiment. We will simulate two different configurations, first, assuming that there is no initial correlation between coils, and second, assuming a correlation coefficient of $\rho = 0.1$. From the data, and using the

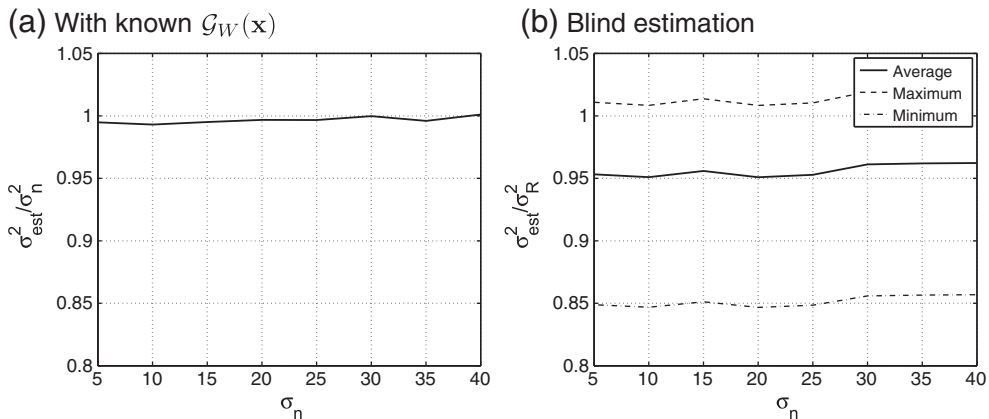


Fig. 3. Estimation of the variance of noise from SENSE. The average of 100 experiments is considered.

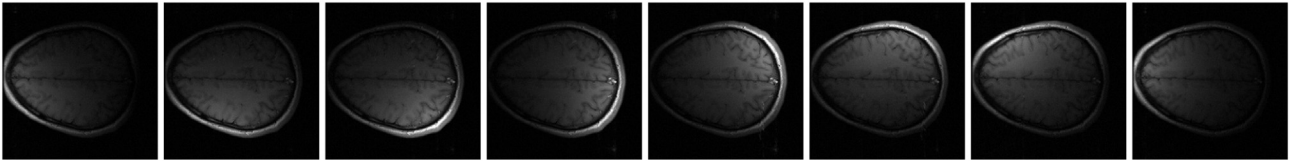


Fig. 4. Slice from a brain T1 acquisition done in a GE Signa 1.5 T EXCITE with 8 coils.

theoretical expression in Eq. (9) we calculate the variance of noise for each pixel in the final image. In order to test the theoretical distributions, 5000 samples of 8 complex 256×256 Gaussian images with zero mean and covariance matrix Σ are generated. The \mathbf{k} -space of the data is subsampled by a $2 \times$ factor and reconstructed using SENSE and the synthetic sensitivity field. We estimate the variance of noise in each point using the second order moment of the Rayleigh distribution [19]:

$$\sigma_{\mathcal{R}}^2(\mathbf{x}) = \frac{1}{2} E\{M^2(\mathbf{x})\}.$$

We estimate the $E\{M^2(\mathbf{x})\}$ along the 5000 samples.

Visual results are depicted in Fig. 2. For the synthetic maps, when no correlations are considered, the final variance of noise will not depend on the position \mathbf{x} . Therefore, in this particular case $\sigma_{\mathcal{R}}^2(\mathbf{x}) = \sigma_{\mathcal{R}}^2$. The estimated values in Fig. 2-(b) show a noise pattern that slightly varies around the real value (note the small range of variation). In this very particular case, the noise can be considered to be spatially stationary, and the final image (leaving the correlation between pixels aside) is equivalent to one obtained from a single-coil scanner.

When correlations are taken into account, even using the same synthetic sensitivity map, results differ. In Fig. 2-(c), the theoretical value shows that the standard deviation of noise of the reconstructed data is not the same for every pixel, i.e., the noise is no longer spatial-stationary. The center of the image shows a larger value that decreases going north and south. So, in this more realistic case, the $\sigma_{\mathcal{R}}^2(\mathbf{x})$ will depend on \mathbf{x} , which can have serious implications for future processing, such as model based filtering techniques. The estimated value in Fig. 2-(d) shows exactly the same non-homogeneous pattern across the image. In the last experiment, Fig. 2-(e) and Fig. 2-(f), a real sensitivity map is used, and correlation between coils is also assumed. Again, the noise is non-stationary. To increase the dynamic range of the images, the logarithm has been used to show the data.

Secondly, we will validate the noise estimation capability of the proposed method by carrying out an experiment with a 2D synthetic slice from a BrainWeb MR volume [28], with intensity values in $[0 - 255]$. The average intensity value for the White Matter is 158, for the Gray Matter is 105, for the cerebrospinal fluid 36 and 0 for the background. An 8-coil system is simulated using the artificial sensitivity in Fig. 1. Image in each coil is corrupted with additive circular complex Gaussian noise with std σ_n ranging in $[5 - 40]$ and $\rho = 0.1$ between all coils. The \mathbf{k} -space is uniformly subsampled by a factor of 2 and reconstructed using SENSE. Note that the variance of noise of the subsampled images in each coil is amplified by a factor r [12]: $(\sigma_n^2)_{\text{sub}} = r \times \sigma_n^2$.

Results for the experiment are shown in Fig. 3-(a): the average of the 100 experiments divided by the actual value of σ_n^2 is depicted. Accordingly, the closer to 1, the better the estimation. From the figure it can be seen that the estimation is very accurate for all the considered values of σ_n . The estimation is similar to the one carried out for single coil data in [4]. However, the goodness of the estimation lies in the fact that the sensitivity maps are available. We repeat the estimation assuming that the maps are not available, and considering a single $\sigma_{\mathcal{R}}^2$ value for the whole image:

$$\widehat{\sigma_{\mathcal{R}}^2} = \frac{1}{2} \text{mode}\left\{\left\langle M_L^2(\mathbf{x}) \right\rangle_{\mathbf{x}}\right\} \quad (36)$$

We define the ratio $\widehat{\sigma_{\mathcal{R}}^2}/\sigma_{\mathcal{R}}^2(\mathbf{x})$ and we calculate the average, the minimum and maximum values across the image, and the average along 100 samples. Results are depicted in Fig. 3-(b). The estimated value presents a constant bias of around 5% for all values. The estimated value will be in a range from 85% to 100% of the original value. Hence, if $\mathcal{G}_W(\mathbf{x})$ is unknown, estimating an individual value of σ_n^2 will only be acceptable for certain applications, whenever they are robust enough to cope with a bit deal of bias and a higher deal of uncertainty in this parameter.

Finally, an experiment is carried out with data from a real acquisition, see Fig. 4, with sensitivity map in Fig. 1-bottom. First, as a

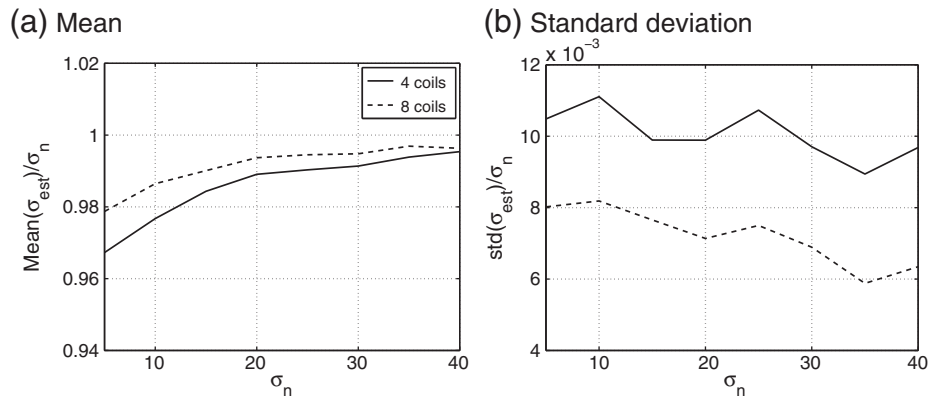


Fig. 5. Results of σ_n estimation using the proposed method; 100 experiments are considered for each sigma value. (a) Mean of the estimated value divided by the actual value. (b) Standard deviation of the estimated values.

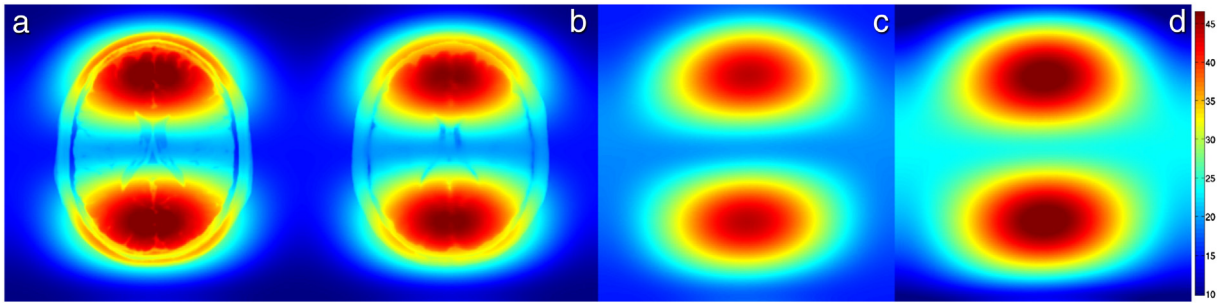


Fig. 6. Effective standard deviation of noise: (a) Original $\sigma_{\text{eff}}(\mathbf{x})$, derived from the GRAPPA weights and Eq. (14); (b) Estimated $\hat{\sigma}_{\text{eff}}(\mathbf{x})$ from Eq. (35); (c) Estimation of effective std of noise for SNR = 0, $\hat{\sigma}_{\text{eff,B}}(\mathbf{x})$; (d) Estimation of effective std of noise for high SNR, $\hat{\sigma}_{\text{eff,S}}(\mathbf{x})$.

golden standard, parameter σ_n is estimated from the Gaussian complex data:

Real component	$\hat{\sigma}_n = 4.1709$
Imag. component	$\hat{\sigma}_n = 4.0845$

Then a subsampled acquisition is simulated and reconstructed with SENSE. σ_n is first estimated using Eq. (28) and then, assuming the map $\mathcal{G}_W(\mathbf{x})$ is unknown, using Eq. (36). Results are as follows:

Magnitude ($\mathcal{G}_W(\mathbf{x})$ known)	$\hat{\sigma}_n/\sqrt{r} = 4.1728$
Magnitude ($\mathcal{G}_W(\mathbf{x})$ unknown)	$\hat{\sigma}_n/\sqrt{r} = 4.8404$

Note that the value estimated using the proposed method is totally consistent with the estimation done over the original complex Gaussian data. The blind estimation method, on the other hand, overestimates the noise level. This is caused because in Eq. (29) the map given by $\mathcal{G}_W(\mathbf{x})$ is basically a normalization. The lack of knowledge of this parameter displaces the mode of the distribution from its actual value, hence the mismatch. However, for some applications in which a great accuracy is not needed, there could still be a valid value that gives a rough approximation to the variance of noise.

4.2. Noise estimation in GRAPPA

For the sake of validation, several experiments are considered. **First**, synthetic experiments were carried out using the same 2D synthetic slice from a BrainWeb MR volume used for SENSE. Image in each coil is again corrupted with Gaussian noise with std σ_n ranging in [5 – 40] and $\rho = 0$. The \mathbf{k} -space is uniformly subsampled by a factor of 2, keeping 32 ACS lines. The CMS is reconstructed using GRAPPA and SoS. The sample local moments have been calculated using 7×7 neighborhoods. Two different cases are considered in the simulation, 4 and 8 coils.

Results for the experiment are shown in Fig. 5: in Fig. 5-(a), the mean of the 100 experiments divided by the actual value of σ_n is depicted. Accordingly, the closer to 1, the better the estimation; in Fig. 5-(b), the standard deviation of the experiments divided by the actual value is shown; the lower the value, the better the estimation.

From the results it can be seen that the estimation is very accurate, although a small bias appears for low values of σ_n . This bias is surely motivated by a mismatch between the GRAPPA reconstructed image and the nc- χ model: according to [16] the error of approximating the CMS by a nc- χ is larger for very low σ_n values. All in all, the proposed method shows a very good average behavior – the values are in a small range between 0.97 and 1 – with a small biased mean and a very low variance, which assures a consistent estimation.

For the sake of illustration, the map of the effective values of noise is also calculated for one single experiment with $\sigma_n = 10$. For that

experiment, the theoretical value of $\sigma_{\text{eff}}^2(\mathbf{x})$ is calculated using Eq. (14). From the expression in Eq. (35), using the estimated noise $\hat{\sigma}_n$ and the GRAPPA weights coded in θ , the variance of noise for the two extreme cases (SNR = 0 and high SNR) is estimated. Using the correction factor $\hat{\phi}_n(\mathbf{x})$, a global value for $\sigma_{\text{eff}}^2(\mathbf{x})$ is obtained.

Results are depicted in Fig. 6-(a) ($\sigma_{\text{eff}}(\mathbf{x})$); Fig. 6-(b) ($\hat{\sigma}_{\text{eff}}(\mathbf{x})$); Fig. 6-(c) ($\hat{\sigma}_{\text{eff,B}}(\mathbf{x})$); Fig. 6-(d) ($\hat{\sigma}_{\text{eff,S}}(\mathbf{x})$). The correction factor $\hat{\phi}_n(\mathbf{x})$ is depicted in Fig. 7.

From the illustrations it is easy to see that the variance of noise has a high variation itself across the image. $\sigma_{\text{eff}}(\mathbf{x})$ ranges from 10 to 45. Even inside the same tissue, there is a huge variation (from 25 to 45). There is, also, a high mismatch between the head and the background areas. Some interesting conclusions can be raised from this: (1) The assumption of a single σ_n^2 value for the whole volume does not hold in GRAPPA. Assuming this single value will clearly bias any further processing; (2) In this example, the noise values in the background are much smaller than those inside the tissue. If the background is used to estimate the noise, and no correction is applied, there can be a huge mismatch between the real noise and the estimated value.

For the **second** experiment, real acquisitions are considered. 100 repetitions of the same slice of a phantom, scanned in an 8-channel head coil on a GE Signa 1.5 T EXCITE 12m4 scanner with FGRE Pulse Sequence to generate low SNR, see Fig. 8 `efimag:ball`. Matrix size = 128×128 , TR/TE = 8.6/3.38 ms, FOV 21×21 cm, slice thickness = 1 mm. Noise variance σ_n^2 is initially estimated using the variance of the real part of every coil of every sample, where the noise is known to be additive Gaussian [29]. This value σ_n^2 is taken as

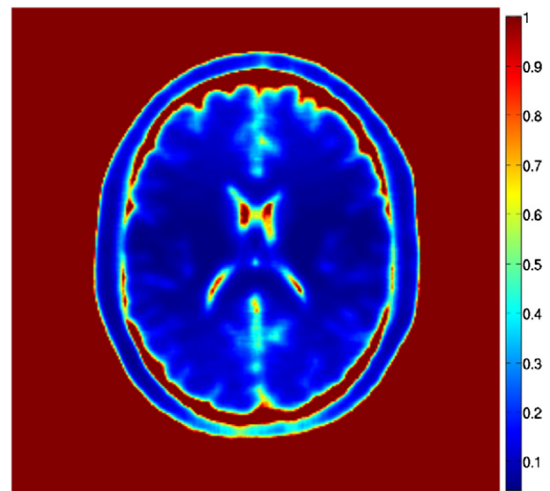


Fig. 7. Estimation of correction factor $\hat{\phi}_n(\mathbf{x})$ from Eq. (34).

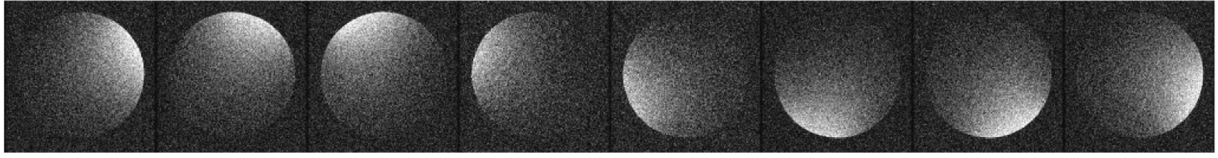


Fig. 8. Slice of an 8-coil 2D acquisition of the phantom used for the experiments.

Golden Standard. Then, all the 100 samples are $2 \times$ subsampled. The GRAPPA reconstruction coefficients are derived from one sample, using 32 ACS lines, and used for interpolation in all samples. The CMS is obtained by SoS. Noise is estimated over each CMS using Eq. (28). For the sake of illustration, values for $\text{tr}(\Theta)(\mathbf{x})$ derived from the GRAPPA coefficients are depicted in Fig. 9. (See Fig. 8.)

Estimation results are as follows:

σ_0	mean $\{\hat{\sigma}_n\}$	mean $\{\hat{\sigma}_n\}/\sigma_0$	std $\{\hat{\sigma}_n\}/\sigma_0$
0.0428	0.0424	0.9905	0.0113

Results obtained estimating the noise with the proposed method are totally consistent with the value obtained over the complex Gaussian images without subsampling. There is a very small bias in the estimation and the method also shows a very small variance, as also seen in the synthetic experiments. The map of $\text{tr}(\Theta)(\mathbf{x})$ depicted in Fig. 9 shows that, in this real case, there is also a great variation of the noise parameter across the image.

Finally, for the sake of comparison with SENSE estimation, a new experiment is carried out with the data from the real acquisition in Fig. 4, as a golden standard for parameter σ_n the estimation from the Gaussian complex already done for SENSE ($\hat{\sigma}_n = 4.1709$ for the real component.) The complex data are subsampled with $r = 2$. The \mathbf{k} -space is reconstructed using GRAPPA and 32 ACS lines and the CMS is obtained by SoS. Noise is estimated over the CMS using Eq. (28). Two different estimations have been done: (1) using the GRAPPA coefficients; (2) assuming the coefficients unknown. In the last case, matrix $\Theta(\mathbf{x})$ is replaced by an 8×8 identity matrix.

Results are as follows:

Magnitude (GRAPPA coefficients known)	$\hat{\sigma}_n \times \sqrt{r} = 4.1097$
Magnitude (GRAPPA coefficients unknown)	$\hat{\sigma}_n \times \sqrt{r} = 5.1933$

Again, like in SENSE; the value estimated using the proposed method is consistent with the estimation done over the original complex Gaussian data. The blind estimation method, on the other hand, overestimates the noise level. Note that there is a great lack of

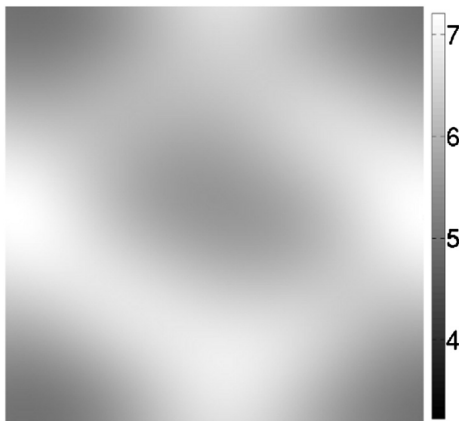


Fig. 9. Values of map $\text{tr}(\Theta)(\mathbf{x})$ from the GRAPPA reconstruction coefficients of the second experiment.

knowledge of a normalization level, hence the error. However, note that it can still be valid to estimate the order of magnitude of the variance of noise, or in case a rough estimation is needed.

5. Conclusions

The proper modeling of the statistics of thermal noise in MRI is crucial for many image processing and computer aided diagnosis tasks. While the stationary Rician and nc- χ models have been the keystone of statistical signal processing in MR for years, the stationarity assumption cannot be applied when parallel imaging reconstruction is considered: the main assumption of a single value of σ_n^2 to characterize the whole data set is no longer valid. When pMRI techniques are used, due to the reconstruction process, the variance of noise becomes \mathbf{x} -dependent, with a different value for each pixel.

To overcome the problems of non-stationarity, we have proposed a novel noise estimation technique to be used with SENSE and GRAPPA reconstructed data. The estimation of the spatially variant $\sigma_n^2(\mathbf{x})$ is of paramount importance, since the knowledge of this parameter will allow us to re-use many of the methods proposed in literature for stationary models. In most cases it will suffice with changing an scalar σ_n^2 value by the spatially dependent $\sigma_n^2(\mathbf{x})$.

The estimation methods proposed have shown to be accurate, robust and easy to use. However, it also shows some limitations. First, correlation between coils must be known beforehand, as well as the sensitivity map from each coil (in SENSE) or the reconstruction weights (in GRAPPA). Finally, some post processing software in the scanner may add a mask to data, which eliminates part of the background, drastically reducing the number of points available for noise estimation [30]. The estimation method selected must be properly adjusted to this problem. Note that if the background is totally removed, the estimation should be done using methods that do not rely on the background, but on the signal areas.

Acknowledgments

The authors acknowledge Ministerio de Ciencia e Innovación for grant TEC2010-17982 and Centro de Diagnóstico Recoletas for MRI acquisition.

References

- [1] Huang H, Zhang J, van Zijl PC, Mori S. Analysis of noise effects on DTI-based tractography using the brute-force and multi-ROI approach. *Magn Reson Med* 2004;52(3):559–65.
- [2] Gudbjartsson H, Patz S. The Rician distribution of noisy MRI data. *Magn Reson Med* 1995;34(6):910–4.
- [3] McGibney G, Smith M. Unbiased signal-to-noise ratio measure for magnetic resonance images. *Med Phys* 1993;20(4):1077–8.
- [4] Aja-Fernández S, Alberola-López C, Westin C-F. Noise and signal estimation in magnitude MRI and Rician distributed images: a LMMSE approach. *IEEE Trans Image Process* 2008;17(8):1383–98.
- [5] Brummer M, Mersereau R, Eisner R, Lewine R. Automatic detection of brain contours in MRI data sets. *IEEE Trans Med Imaging* 1993;12(2):153–66.
- [6] Dolui S, Kuurstra A, Michailovich OV. Rician compressed sensing for fast and stable signal reconstruction in diffusion MRI. In: Haynor DR, Ourselin S, editors. *Medical imaging 2012: image processing*, vol. 8314, SPIE; 2012.
- [7] Noh J, Solo V. Rician distributed fMRI: asymptotic power analysis and Cramer–Rao lower bounds. *IEEE Trans Signal Process* 2011;59(3):1322–8.

- [8] Schmid VJ, Whitcher B, Padhani AR, Taylor NJ, Yang G-Z. A Bayesian hierarchical model for the analysis of a longitudinal dynamic contrast-enhanced MRI oncology study. *Magn Reson Med* 2009;61(1):163–74.
- [9] Constantinides C, Atalar E, McVeigh E. Signal-to-noise measurements in magnitude images from NMR based arrays. *Magn Reson Med* 1997;38:852–7.
- [10] Aja-Fernández S, Tristán-Vega A. Influence of noise correlation in multiple-coil statistical models with sum of squares reconstruction. *Magn Reson Med* 2012;67(2):580–5.
- [11] Aja-Fernández S, Tristán-Vega A, Brion V. Effective noise estimation and filtering from correlated multiple-coil mr data. *Magn Reson Imag* 2013;31(2):272–85.
- [12] Pruessmann KP, Weiger M, Scheidegger MB, Boesiger P. SENSE: sensitivity encoding for fast MRI. *Magn Reson Med* 1999;42(5):952–62.
- [13] Griswold MA, Jakob PM, Heidemann RM, Nittka M, Jellus V, Wang J, et al. Generalized autocalibrating partially parallel acquisitions (GRAPPA). *Magn Reson Med* 2002;47(6):1202–10.
- [14] Dietrich O, Raya J, Reeder S, Ingrisch M, Reiser M, Schoenberg S. Influence of multichannel combination, parallel imaging and other reconstruction techniques on MRI noise characteristics. *Magn Reson Imaging* 2008;26:754–62.
- [15] Thünberg P, Zetterberg P. Noise distribution in SENSE- and GRAPPA-reconstructed images: a computer simulation study. *Magn Reson Imaging* 2007;25:1089–94.
- [16] Aja-Fernández S, Tristán-Vega A, Hoge WS. Statistical noise analysis in GRAPPA using a parametrized non-central chi approximation model. *Magn Reson Med* 2011;65(4):1195–206.
- [17] Sijbers J, den Dekker AJ, Van Dyck D, Raman E. Estimation of signal and noise from Rician distributed data. *Proc. of the Int. Conf. on Signal Proc. and Comm., Las Palmas de Gran Canaria, Spain; 1998*. p. 140–2.
- [18] Sijbers J, den Dekker A, Van Audekerke J, Verhoye M, Van Dyck D. Estimation of the noise in magnitude MR images. *Magn Reson Imaging* 1998;16(1):87–90.
- [19] Aja-Fernández S, Tristán-Vega A, Alberola-López C. Noise estimation in single and multiple coil MR data based on statistical models. *Magn Reson Imaging* 2009;27:1397–409.
- [20] Sijbers J, Poot D, den Dekker AJ, Pintjens W. Automatic estimation of the noise variance from the histogram of a magnetic resonance image. *Physics in Medicine and Biology*, vol. 52; 2007. p. 1335–48.
- [21] Koay CG, Basser PJ. Analytically exact correction scheme for signal extraction from noisy magnitude MR signals. *J Magn Reson* 2006;179:317–22.
- [22] Hoge WS, Brooks DH, Madore B, Kyriakos WE. A tour of accelerated parallel MR imaging from a linear systems perspective. *Concepts Magn Reson Part A* 2005;27A(1):17–37.
- [23] Larkman DJ, Nunes RG. Parallel magnetic resonance imaging. *Phys Med Biol* 2007;52:15–55 [invited Topical Review].
- [24] Robson P, Grant A, Madhuranthakam A, Lattanzi R, Sodickson D, McKenzie C. Comprehensive quantification of signal-to-noise ratio and g-factor for image-based and k-space-based parallel imaging reconstructions. *Magn Reson Med* 2008;60:895.
- [25] Wang Y. Description of parallel imaging in MRI using multiple coils. *Magn Reson Med* 2000;44:495–9.
- [26] Blaimer M, Breuer F, Mueller M, Heidemann R, Griswold M, Jakob P. SMASH, SENSE, PILS, GRAPPA: how to choose the optimal method. *Top Magn Reson Imaging* 2004;15(4):223–36.
- [27] Breuer FA, Kannengiesser SA, Blaimer M, Seiberlich N, Jakob PM, Griswold MA. General formulation for quantitative g-factor calculation in grappa reconstructions. *Magn Reson Med* 2009;62(3):739–46.
- [28] Collins D, Zijdenbos A, Kollokian V, Sled J, Kabani N, Holmes C, et al. Design and construction of a realistic digital brain phantom. *IEEE Trans Med Imaging* 1998;17(3):463–8.
- [29] Aja-Fernández S, Vegas-Sánchez-Ferrero G, Martín-Fernández M, Alberola-López C. Automatic noise estimation in images using local statistics. Additive and multiplicative cases. *Image Vision Comput* 2009;27(6):756–70.
- [30] Aja-Fernández S, Vegas-Sánchez-Ferrero G, Tristán-Vega A. About the background distribution in MR data: a local variance study. *Magn Reson Imaging* 2010;28(5):739–52.